WIPL-D Pro: What is New in v12.0?

Improvements/new features introduced in v12.0 are:

1. Extended - Extreme Limits
   a. Extremely LOW contrast materials
   b. Extended resolution for radiation pattern
   c. Extremely HIGH contrast materials
   d. Extended resolution for near field
   e. Extremely LOW "low frequency break down"
   f. Extended limits: small details-large structures
2. New Generators - User Defined Set of Currents
   a. Excitation of the structure by user defined sets of (electric and/or magnetic) current sources
   b. Creation of set of current sources by exporting current distribution of selected wires / plates
   c. Enabled calculation of near field and radiation due to field/current generators stand alone
   d. Calculation of near field / radiation pattern due to selected wires and plates
3. Highly efficient simulation of huge multi-layered radomes excited by arrays of field generators.
4. Local Settings for Selected Entities:
   a. Max patch size
   b. Reference frequency
   c. Unused entities
5. Parallelization
   a. Improved multi-core CPU parallelization of matrix fill - efficiency up to 97 % for 20 cores
   b. Parallelization of excitation and near/far field calculations due to field generators
6. Improved specification of distributed loadings: assignment to objects/groups (not only wires & plates) and ability to copy and re-numerate them
7. User defined data files for frequency dependent symbols (e.g. frequency dependent materials)
8. Calculation of specific absorption (SA) through integration with WIPL-D Time Domain Solver
9. Minor options/improvements
   a. "Set as read-only" option for project
   b. Improved field generators functionality in presence of PEC/PMC plane
   c. Disable/enable near filed and radiation pattern calculations via button
   d. Silent run (hides kernel window)
   e. Graphical representation of surface currents in logarithmic scale (dBμ).
   f. Circular axes in graphical representation of 3D radiation pattern.

g. Enabled optimization of absolute gain, VSWR, etc. in WIPL-D Optimizer)

1. Extended - Extreme Limits

Extended-extreme limits are enabled by new generation of integration methods for highly accurate calculation of MoM matrix elements combined with advanced matrix equilibration to balance source/field quantities and basis/test functions in MoM solution.

a) Extremely LOW contrast materials

Define the relative difference in permittivity and permeability, δ_e and δ_m with respect to vacuum as

$$\delta_e = |\varepsilon_r - 1| \quad \delta_m = |\mu_r - 1|$$

Relative differences down to 10^{-6} can be distinguished by EM simulation in v12.0. (Previous version could only distinguish differences down to 10^{-3}.)

Consider dielectric sphere of 1λ diameter illuminated by θ-polarized plane wave. RCS in *xOy*-plane for relative electric constant decreasing from $\varepsilon_r = 1.1$ down to $\varepsilon_r = 1.000001$ is compared with those for PEC sphere and sphere filled by vacuum (see Fig. 1).
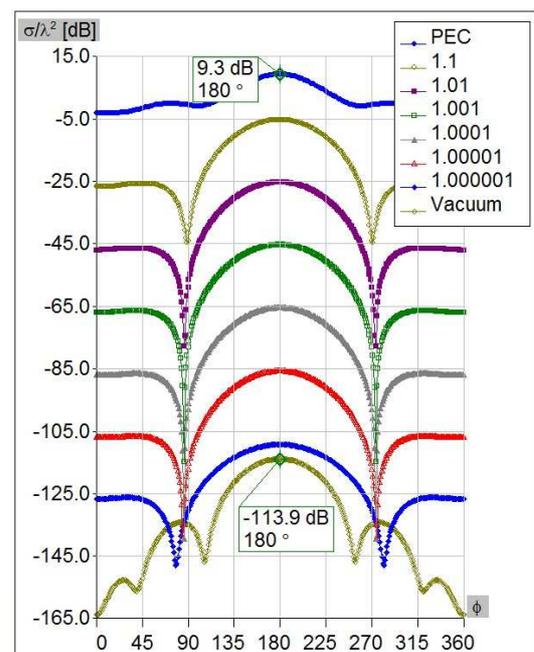

Fig. 1. RCS of dielectric sphere with relative electric constant going from 1.1 down to 1.000001 compared with those of PEC and vacuum filled spheres.

b) Extended resolution for radiation pattern

Resolution of radiation pattern is determined as difference between maximum values of RCS obtained for PEC and vacuum filled spheres. According to Fig. 1 these maximum values are 9.3 dB and -113.9 dB, respectively. Using these valuse the resolution is detetrmined to be 123.2 dB. (Previous version had resolution less than 70 dB.)

c) Extremely HIGH contrast materials

Relative differences in permittivity and permeability, δ_e and δ_m up to 10^{+6} can be distinguished by EM simulation in v12.0. (Previous version distinguished differences up to 10^{+4}.)

Metallic sphere (1λ diameter), excited by θ-polarized plane wave incoming along (-*x*)-axis, is analyzed at *f* = 300 MHz as lossy material (dielectric) sphere of relative electric constant $\varepsilon_r = 1 - j10^m$, *m* = 1,...,6. Fig. 2 shows near electric field along *y*-axis in dBs with respect to µV/m.

It is seen that electric field down to -780 dBµ can be calculated, which is -900 dBµ with respect to the maximum value at the sphere surface. It corresponds to ~100 skin effect depths.
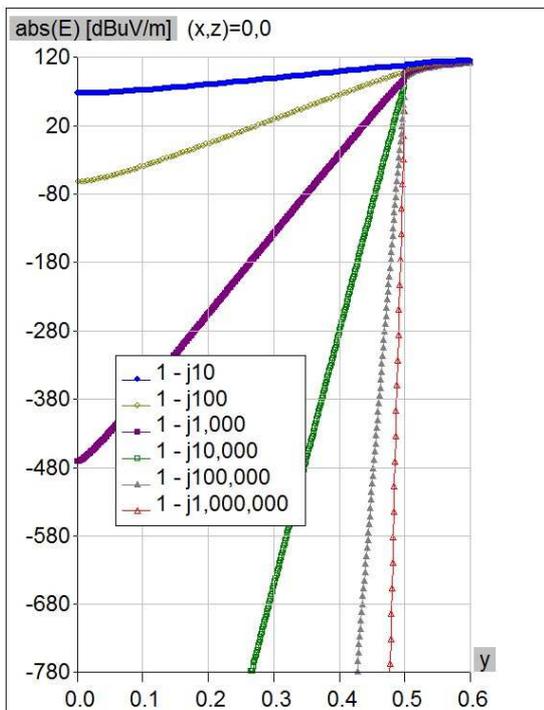

Fig. 2. Near electric field along y-axis of metallic (lossy material) sphere (1m diameter) for relative electric constant
$$\varepsilon_r = 1 - j10^m, \ m = 1,2,3,4,5,6.$$

d) Extended resolution for near field

Resolution of near field is calculated as difference between maximum value and minimum value of the field that can be determined in case of field penetration into lossy material body. Referring to the results shown in Fig. 2, this resolution is found to be 900 dBµ. (Previous version has resolution of ~150 dBµ.)

e) Extremely LOW "low frequency breakdown"

PEC sphere and dielectric sphere of (1m diameter) are illuminated by linearly polarized plane wave. Fig. 3 shows monostatic RCS versus frequency, from 1 Hz to 100 MHz. Unstable results are observed only at frequencies of few Hz. (Previous version would show instability even at few KHz.)
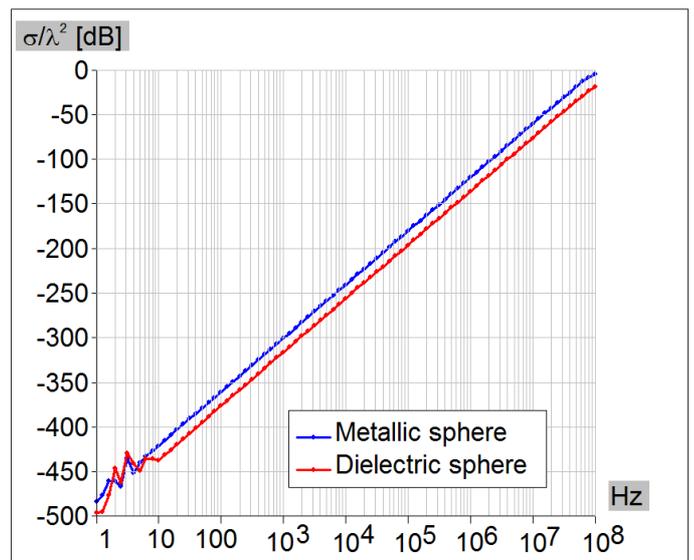

Fig. 3. RCS of metallic/dielectric sphere (1m diameter) versus frequency from 1Hz to 100 MHz.

f) Extremely small details at large structures

Previous example shows that v12.0 can handle extremely small patches. Thus, at frequency of 15 Hz the patch size is ~$10^{-8}\ \lambda$. Such small patches can be used to model some very important small details in large EM scenarios.

As an example, consider a small PCB antenna shown in inset B of Fig. 4. Basically, the antenna is simulated taking into account thin coaxial line 100 mm long, as shown in inset A. However, for good agreement with measured results, modeling of full measurement scenario is needed (see Fig. 4).

Fig. 4. Small PCB antenna in measurement scenario: EM model (up) and photography (down)
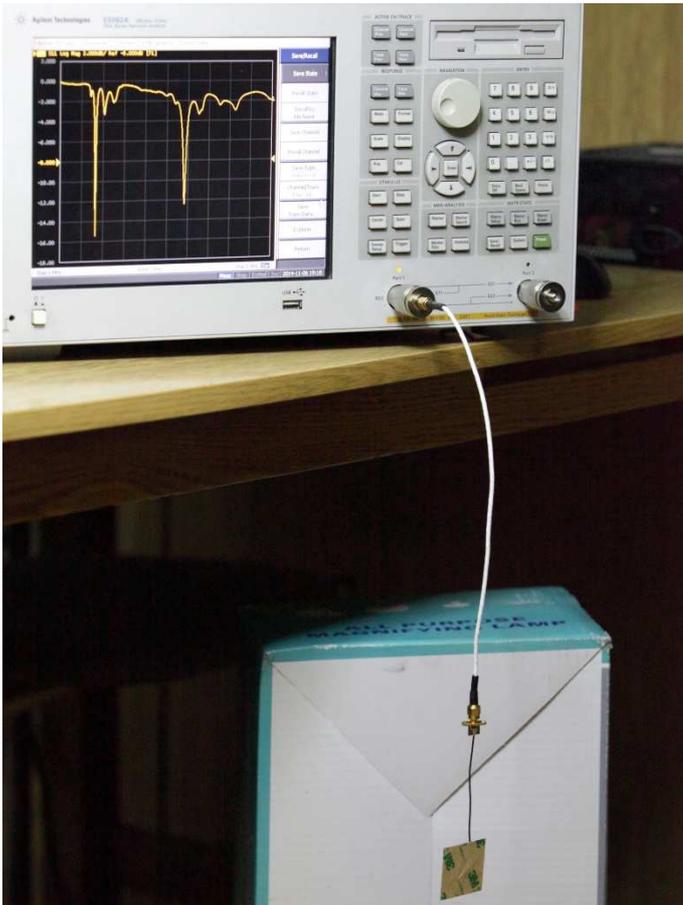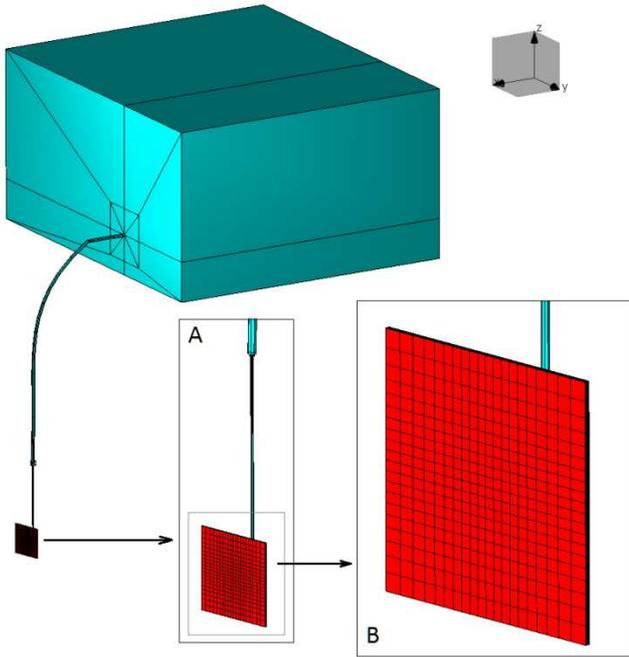
Fig. 5 shows s_{11} parameter in range of 200 MHz to 600 MHz. Good agreement between simulation and measurements is observed in case when full scenario is simulated. (It is understandable having in mind that the antenna has no balun.)

Fig. 6 shows s_{11} parameter in range of 2 MHz to 2 GHz. Maximum dimension of this scenario is 0.77 m. Radius of thin coaxial line is 0.164 mm. Thus, the maximum size of the scenario looking in the full frequency range exceeds 5 λ, while small details are as small as $\lambda/1,000,000$.
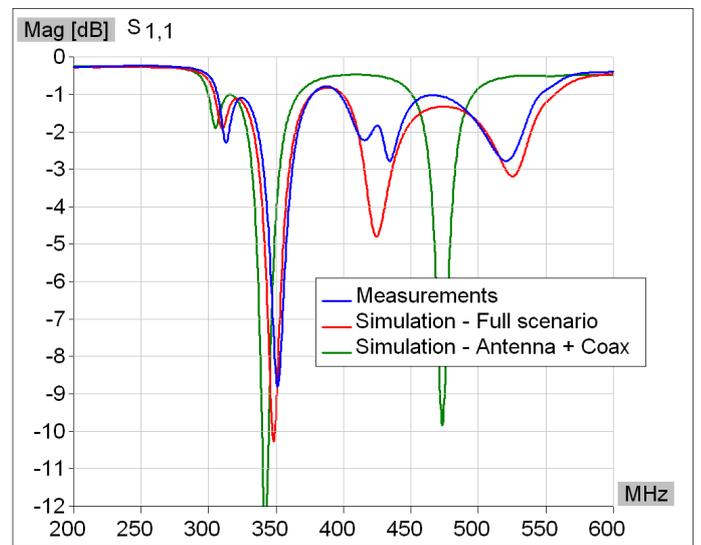

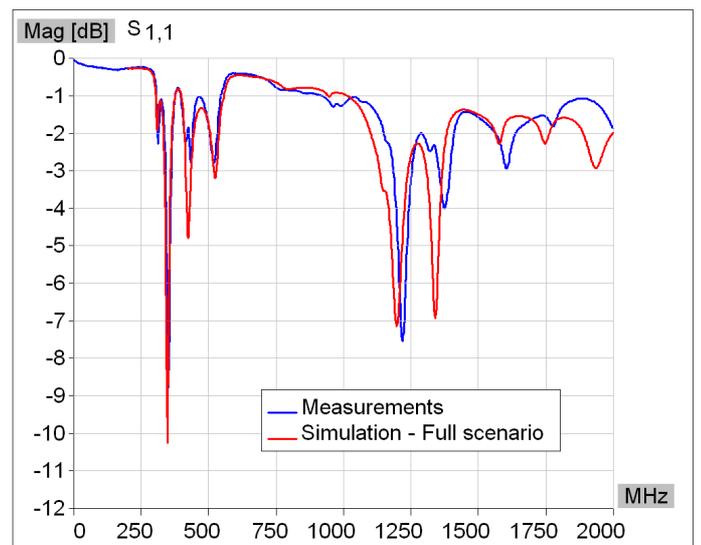Fig. 5. S11 versus frequency for small PCB antenna: two simulation sets compared with measurement.

Fig. 6. S11 for small PCB antenna compared with measurements in wide frequency range.

2. New generators - User defined sets of currents

Current generator is a new type of generator consisting of arbitrary user defined set of electric and/or magnetic currents spread along straight linear segments and/or quadrilaterals (bilinear surfaces). Current generator is defined by ASCII files written in format explained in details in the manual, so that these files can be created outside WIPL-D environment. They can also be created by exporting currents for selected wires and plates from arbitrary project run by 3D EM Solver. Once created, current generator can be either used to excite arbitrary structure, or run as a standalone to calculate near and/or far field distribution.

A plenty of possibilities offered by this new type of generator will be demonstrated on example of Cassegrain reflector (25.5λ in diameter) fed by circular waveguide feeder, as shown in Fig. 7.
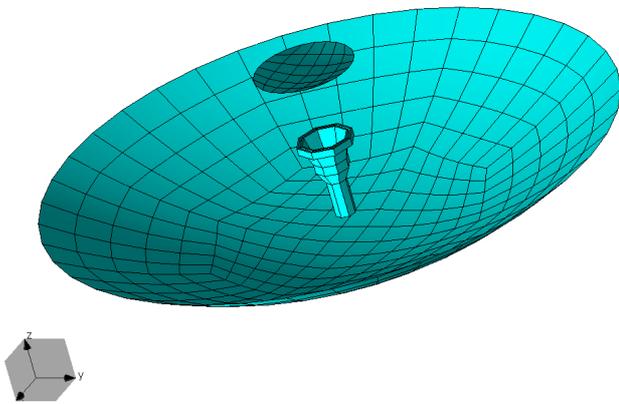

Fig. 7. Cassegrain reflector antenna (25.5 λ in diameter) fed by circular waveguide feeder

a) Creation of set of current sources by exporting current distribution of selected wires / plates

Circular waveguide feeder, shown in cyan color in Fig. 8, is simulated standalone. Currents distributed over all wires and plates in the model are exported into files that define current generator. Once such current generator is imported into new project, it appears in a preview as shown in gray color in Fig. 8. Radiation pattern due to such current generator, which is shown in Fig. 8., is practically the same as in original project.
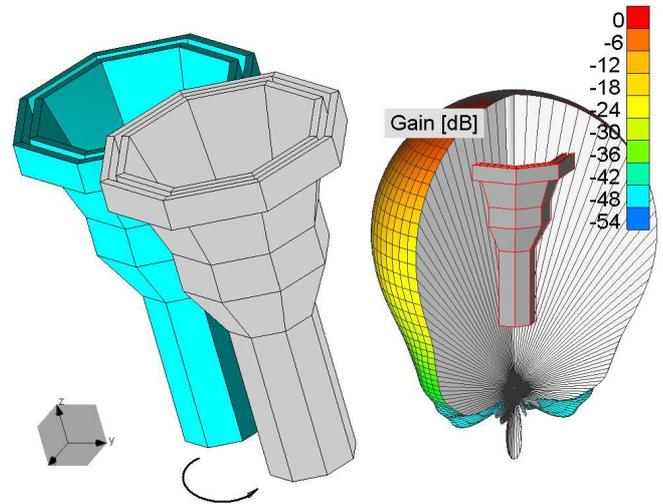

Fig. 8. Radiation pattern due to current generator (shown in gray), obtained by exporting currents from feeder project (shown in cyan)

c) Excitation of the structure by user defined sets of (electric and/or magnetic) current sources

Instead of original feeder shown in Fig. 7, the corresponding current generator can be used, as shown in Fig. 9. Using such feeder reduces the number of unknowns to be solved. Fig. 10 compares radiation pattern of Cassegrain antenna obtained by using original feeder and corresponding current generator. Difference can be explained by the fact that current generator does not take into account coupling between the feeder and reflectors.
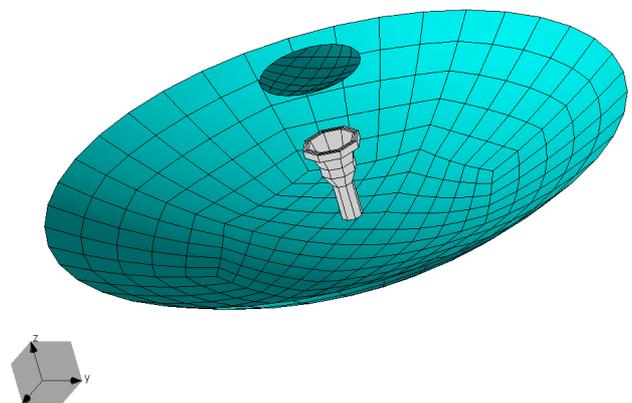

Fig. 9. Cassegrain reflector antenna fed by current generator (shown in gray)
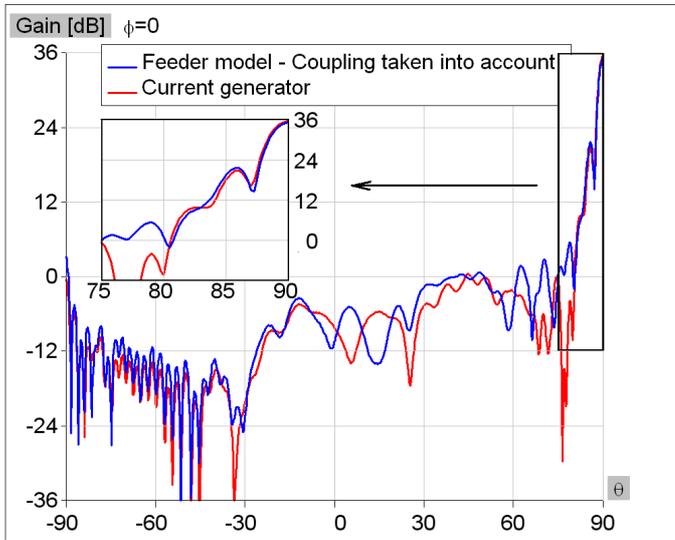
Fig. 10. Radiation pattern of Cassegrain antenna obtained by current generator compared to that obtained by original feeder structure

c) Calculation of near field / radiation pattern due to selected wires and plates

In order to calculate the contribution of paraboloidal reflector to radiation pattern of Cassegrain antenna, the currents of reflector antenna are exported into separate current generator, as shown in inset of Fig. 11. Radiation pattern due to such current generator is compared with radiation of full Cassegrain antenna in Fig. 11. It is seen that feeder and subreflector has significant impact on full pattern.
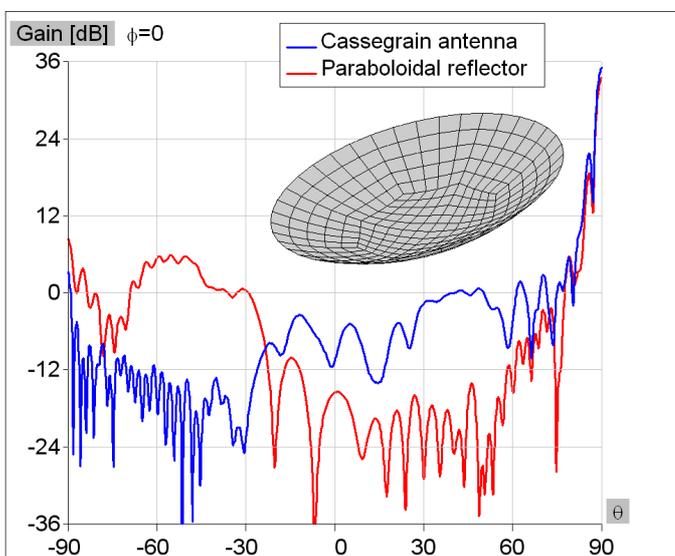

Fig. 11. Radiation pattern due paraboloidal reflector is compared with that of full Cassegrain antenna.

d) Enabled calculation of near field and radiation due to field/current generators stand alone

Radiation patterns due to current generators shown in Figs. 8 and 11 are obtained running the project containing no entities except the current generator itself. Similarly, one can run the project containing the field generator and no other entities. In the previous version only projects containing at least one wire or one plate entity could be run.

3. Highly efficient simulation of huge multi-layered radomes fed by arrays of field generators

Radomes are usually designed to be as much transparent as possible. It means that a wave going from antenna is mostly transmitted, and that only a small part of this wave is reflected back. Further reflections of this wave can be neglected. Moreover, parts of the reflector that are hit with sidelobes, carrying very small amount of energy, need not to be taken account. The user can choose **Power factor** (percentage of energy carried by antenna wave, for which the part of the radome would be taken into account), and in such manner decrease the size of the problem.

As an example let us consider array of 20 by 4 field generators (radiators) in yOz-plane mutual spaced by λ/2, where each radiator emulate radiation of patch antenna in front half space.

Let the array illuminate a relatively thick radome of 22λ in diameter and 27.7λ in height, as shown in Fig. 12. The total number of unknowns for full model is 265,660 and simulation time ~5 hours. Usage of two symmetry planes (colored in light pink and light cyan) reduces number of unknowns 4 times. Decreasing the reference frequency for 40%, further reduces the number of unknowns for 60%. Finally, setting the **Power Factor** to 95% (patches shown in yellow are omitted from simulation), the total number of unknowns is reduced to 15,405, and simulation time to less than 2 minutes.

Figure 13. shows the results for array with reduced radome compared with those with full radome and array stand alone.
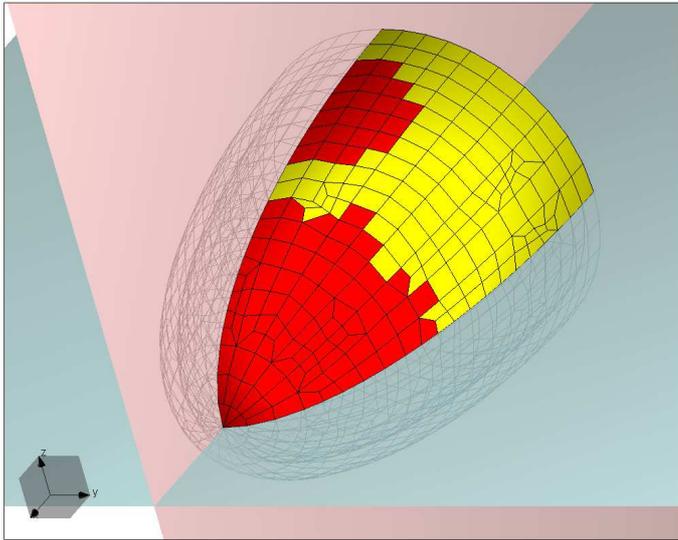

Fig. 12. Model of radome with 2 symmetry planes. Setting **Power factor** to 95% the yellow patches are automatically omitted from simulation.
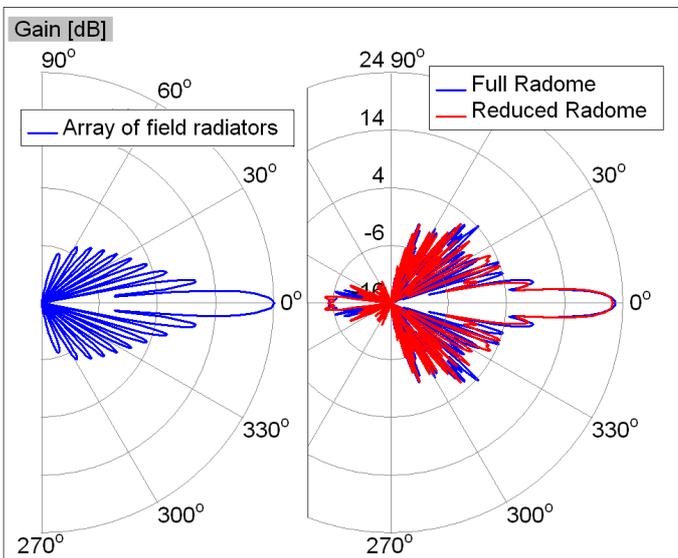

Fig. 13. Radiation pattern of array with reduced radome are compared with those of full radome and array stand alone.

4. Local Settings for Selected Entities

Various local settings can be defined for selected entities (wires, plates, objects, and groups). In particular, it is possible to check "all wires" or "all plates", and specified if local setting are copied or not with coping the entities.

When the structure is modified, the local setting is modified accordingly.

a) Max patch size (MPS)

Enables local modification of max patch size. For example, in case of small PCB antenna in full scenario (Figs. 4 and 5), the global setting of MPS = 0.02λ result in 21,883 unknowns. Local setting of MPS = 1λ applied to measurement setup reduced the number of unknowns to 12,168.

b) Reference frequency

Enables local modification of reference frequency. For example, consider radome fed by array of field generators (Fig. 12). If array of field generators would be replaced by array of patch antennas, the reference frequency decreased globally for the whole structure would produce inaccurate solution. The reason is that such decrease is OK for radome, but not for patch antennas. To reduce the number of unknowns on the radome part, it would be enough to decrease reference frequency locally, for the radome only.

c) Unused entities

Enables selected patches are omitted from simulation, without the need to delete them from the project. For example, consider radome fed by array of field generators (Fig. 12). The patches colored in yellow are simple omitted from simulation, although they are not deleted from the project.

5. Parallelization

a) Improved CPU parallelization of matrix fill

New algorithm for parallelization at multi-core CPU is implemented. The new algorithm provides efficiency up to 97% in case of problem with large number of unknowns. The algorithm is tested up to 20 cores. For example, in case of 20 cores exactly, the matrix fill is accelerated ~19 times when compared to that performed at single core. Turning on the hyper-threading can cause further acceleration of up to 1.5 times. (Previous version provided efficiency of ~90% for 4 cores, and ~70% for 8 cores.)

When higher order bases are used the CPU parallelization of matrix fill outperforms the GPU parallelization whenever the number of cores is higher than 8. The most efficient simulation is achieved combining CPU parallelized matrix fill with GPU parallelized matrix solve. For example, using 20 cores and 1 GPU card the small PCB antenna in full scenario (Figs. 4 and 5) is simulated in 1 minute at a single frequency.

c) Parallelization of excitation and near/far field calculations due to field generators

Calculation of excitation and near/far field due to field generators becomes very time consuming when huge arrays of field sources are applied. These calculations are now parallelized and tested up to 20 cores, which enables effective usage of arrays of up to 100,000 field generators.

6. Improved specification of distributed loadings

In previous version distributed loadings are added to wires and plates after geometrical modeling of the structure is finished. If later the project was modified definition of distributed loadings was not adjusted automatically, so that modification had to be done manually.

In v12.0 distributed loading can be assigned to selected entities (wires, plates, objects and groups). In particular, it is possible to check "all wires" or "all plates", and specified if distributed loadings are copied or not with coping the entities. When the structure is modified the distributed loadings are modified accordingly.

7. User defined data files for frequency dependent symbols

From previous version user could define symbols dependent on frequency, where dependence is specified analytically in the list of symbols. Such option enabled both, EM modeling of frequency dependent materials and modeling of reconfigurable antennas, whose structure depends on frequency. In v12.0 it is enabled that frequency dependence of symbols can be set in user defined files.

In v12.0 it is enabled that frequency dependence of symbols can be set by user defined files.

8. Calculation of specific absorption

Specific absorption (SA) represents EM energy per unit mass deposited in lossy material due to given time varying EM field. Calculation of SA in specified grid of points is enabled through integration with WIPL-D Time Domain Solver.

9. Minor options/improvements

a) "Set as read-only" option for project

The project can be set as "read-only", so that the project cannot be accidentally modified and run, i.e., the project (geometry, excitation, results, etc.) is preserved as it is.

b) Improved field generators functionality in presence of PEC/PMC plane

In previous software versions when PEC/PMC plane was defined in the project, image of field generators had to be defined manually. In the new version of WIPL-D this image is automatically created by WIPL-D kernel, and user has not to take care about that.

c) Disable/enable near filed and radiation pattern calculations via button

Once the grid of near field points and/or far field directions is specified, a user can turn off/on these specifications via button. In previous version it was not possible to automatically restore these specifications once they are reset to default.

d) Silent run

Bu default, during running the project the DOS window pops up, showing the current status of the run. Turning on the "Silent run" option disables the DOS window to pop up. This option is particularly useful in the case of optimizing or sweeping small projects, when the DOS window pops up and closees in a fraction of second for each new set of optimizing-sweeping parameters.

e) Graphical representation of surface currents in logarithmic scale (dBµ)

Enables presenting magnitude of surface currents in logarithmic scale in dBµ, i.e. in dBs with respect to $1 \mu A / m^2$. (In previous version it was enabled to represent the magnitude of surface currents only in linear scale, i.e. in A / m^2).

f) Circular axes in graphical representation of 3D radiation pattern

For example, circular axes can be added to results originally given in Fig. 8, as shown in Fig. 14.
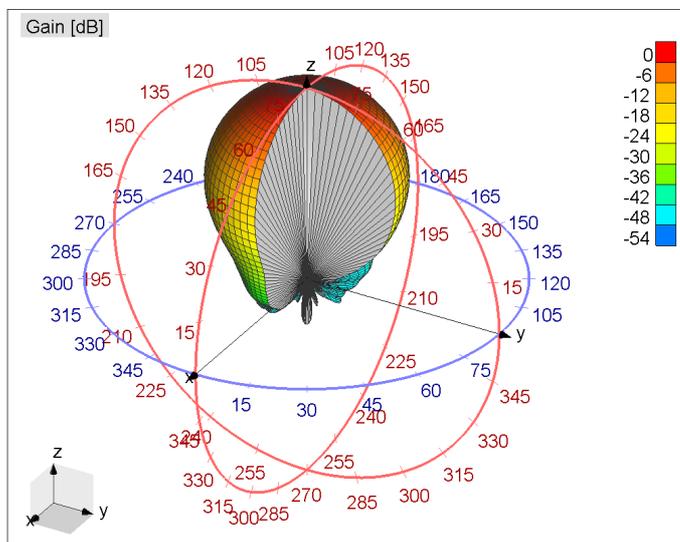

Fig. 14. Circular axes are added to results originally given in Fig. 8.

g) Optimization of recently defined quantities enabled in WIPL-D Optimizer)

Optimization of some quantities, which were added or missing in recent versions of WIPL-D Pro, is now enabled in WIPL-D Optimizer (e.g. VSWR, absolute gain, etc.)